

## Calibration of 5-hole Probe for Flow Angles from Advanced Technologies Testing Aircraft System Flight Data

V. Parameswaran

*National Aerospace Laboratories, Bangalore-560 017*

and

R.V. Jategaonkar

*German Aerospace Centre, Germany*

### ABSTRACT

This paper describes the investigations carried out to calibrate the 5-hole probe for flow angles from advanced technologies testing aircraft system flight data. The flight tests were carried out with gear up and at nominal mid-centre of gravity location for two landing flap positions,  $\delta_f = 1N$  and  $14^\circ$ . Dynamic manoeuvres were executed to excite the short period and Dutch roll mode of the aircraft. In addition, pull up, push down and steady sideslip manoeuvres were also carried out. The data compatibility check on the recorded flight data has been carried out using maximum likelihood output error algorithm to estimate the bias, scale factor, and time delay in the pressure measurements from the 5-hole probe mounted on a noseboom in front of aircraft nose.

Through a way of kinematic consistency checking, flight-validated scale factors, biases, and time delays are determined for the differential pressure measurements for both angle of attack and angle of sideslip. Also, the dynamic pressure measurement is found to have time delays. Based on the earlier investigations, it is once again confirmed that the measurements of attitude angles, obtained from the inertial platform, clearly indicate time delays referred to the other signals like linear accelerations and angular rates which are measured with the dedicated flight instrumentation package.

The identified time delays in attitude angles agreed well with the inertial platform specifications. The estimates of sensitivity coefficients and scale factors from the flight data analysis correlates reasonably well with the manufacturer Rosemount calibration curves for the tested Mach range 0.23-0.53. The flight data analysis at Mach number of about 0.59 indicate Mach dependency for the angle of attack.

**Keywords:** 5-hole probe, parameter estimation method, flight data, flow angle, calibration, flight reconstruction technique, angle of attack, angle of sideslip, ATTAS flight data, Rosemount 5-hole probe, ATTAS test aircraft, flight-validated scale factors, inertial platform specifications, path reconstruction, dynamic pressure measurement, aerodynamic parameters, time delays, pulse code modulation, longitudinal-and lateral-directional motion, analog filters

**NOMENCLATURE**

$a_x, a_y, a_u$	Accelerations along $x, y$ and $z$ body axes	$\dot{p}, \dot{q}, \dot{r}$	Roll, pitch and yaw accelerations
$a$	Velocity of sound	$P_s$	Static pressure
$b_{x,p}, b_{y,p}, b_{u,t}$	Unknown components of $x_0, \Delta z, \Delta u$	$Rg$	Gas constant
$f[.]$	System state function	$R$	Covariance matrix of the residuals
$g$	Acceleration due to gravity	$T_s$	Static air temperature
$g[.]$	System observation function	$T_{tot}$	Total air temperature
$G$	Measurement noise distribution matrix	$t$	Time
$h$	Altitude	$u(t)$	Control input vector
$J$	Cost function	$U$	Time-delayed control input vector
$k$	Discrete time index	$u, v, w$	Velocity components along $x, y$ and $z$ body axes
$K_\alpha, K_\beta$	Sensitivity coefficients for angles of attack and angle of sideslip	$v(t)$	Measurement noise vector
$m$	Number of observation variables	$V$	True airspeed
$Ma$	Mach number	$x$	State vector
$n$	Number of state variables	$X$	Time-delayed state vector
$nz$	Number of time records to be analysed simultaneously	$y$	Observation vector
$N$	Number of data points	$z$	Measurement vector
$p$	Number of control inputs	$\alpha_{Lo}$	Local angle of attack
$P_{\alpha 1}, P_{\alpha 2}$	Pressures at two ports for angle of attack from 5-hole probe	$\beta_{Lo}$	Local angle of sideslip
$P_{\beta 1}, P_{\beta 2}$	Pressures at two ports for angle of sideslip from 5-hole probe	$\beta$	Unknown system coefficients
$p_\alpha$	Differential pressure for angle of attack from 5-hole probe	$\phi, \theta, \psi$	Bank, pitch and yaw angles
$p_\beta$	Differential pressure for angle of sideslip from 5-hole probe	$\rho$	Density of air
$p_{tot}$	Total pressure from 5-hole probe	$\Theta$	Vector of unknown parameters
$P_{dyn}$	Dynamic pressure	$\delta_f$	Landing flap position
$p, q, r$	Roll, pitch and yaw rates	$\Delta t$	Time interval
		$\Delta(.)$	Bias or zero shift in the variables (.)
		$\tau$	Time delay
		$X_a, Y_a, Z_a$	Accelerometer offset distances relative to centre of gravity
		$X_{lo}, Y_{lo}, Z_{lo}$	5-Hole probe (nose boom) offset distances relative to centre of gravity

**SUBSCRIPTS**

0	Initial conditions
<i>a</i>	Accelerometers near the centre of gravity
<i>dyn</i>	Dynamic
<i>l</i>	Index for the time segment
<i>Lo</i>	Local 5-hole probe on a nose boom
<i>m</i>	Measured variable
$\alpha_{Lo}$	Local angle of attack

**1. INTRODUCTION**

Parameter identification is recognised today as the best way to determine aerodynamic parameters from flight test data. Much time of the flight test data analysis was devoted to the calibration of the flow angles using flight path reconstruction techniques. This paper describes the calibration of a 5-hole probe for flow angles from ATTAS flight data.

The ATTAS test aircraft is a modified version of a twin-turbofan, short haul, 44-passenger aircraft of the type VFW-614 manufactured by the Messerschmitt-Bölkow-Blohm, GmbH. The direct lift control flaps can be operated for the landing flap deflections up to 14° in the fly-by-wire mode. Hitherto, the measurements of true airspeed (*V*), angle of attack ( $\alpha$ ), and angle of sideslip ( $\beta$ ) were obtained with a flight log mounted on a boom in front of the aircraft nose. The noseboom minimises the disturbances due to the fuselage interactions.

Due to design considerations, the boom length was limited to about the fuselage diameter in the ATTAS aircraft. The true airspeed was measured using a propeller-driven sensor, whereas two vanes provided the measurements of angle of attack and angle of sideslip<sup>1</sup>. Since the vanes have their own dynamics, it was proposed to replace the flight log with a Rosemount 5-hole probe for the measurements of angle of attack and angle of sideslip<sup>2</sup>. Moreover, 5-hole probe is more robust, reliable and suitable for operation in adverse weather conditions. The 5-hole probe is mounted on a boom in front of the aircraft nose as shown in Fig. 1.



Figure 1. ATTAS aircraft with 5-hole probe

The aim of the present investigation is to flight validate the calibration curves specified by the manufacturer Rosemount obtained from wind tunnel data<sup>2</sup>. The approach is based on the hitherto applied method of flight path reconstruction using parameter estimation method. This, in-turn, requires dynamic manoeuvres with  $\alpha$ , and  $\beta$  variations. A proposed comprehensive flight-test was carried out which included multi-step elevator and rudder input manoeuvres.

**2. DESCRIPTION OF THE 5-HOLE PROBE**

The pressure measurements available from the 5-hole probe are total pressure ( $P_{tot}$ ), differential pressure for angle of attack ( $p_{\alpha 1}$ ), and differential pressure for angle of sideslip, ( $p_{\alpha 1} - p_{\beta 2}$ ). The static pressure ( $p_s$ ) is obtained from the local static ports located at a distance close to the 5-hole pressure ports. Using these pressure measurements, the angle of attack and the angle of sideslip at the sensor location are obtained. The pressure ports<sup>2</sup> of the 5-hole probe are shown in the Fig. 2.

The port ( $p_{tot}$ ) is located in the centre of the sensor head to provide a local pitot pressure source. The differential pressure ( $p_{\alpha 1} - p_{\alpha 2}$ ) is proportional to the product of dynamic pressure ( $p_{dyn}$ ) times local angle of attack ( $\alpha_{Lo}$ ), where the dynamic pressure equals local pitot pressure minus local static pressure ( $p_{tot} - p_s$ ) and ( $\alpha_{Lo}$ ) equals local angle of attack. The local angle of attack ( $\alpha_{Lo}$ ) can be determined according to the relationship<sup>2</sup>

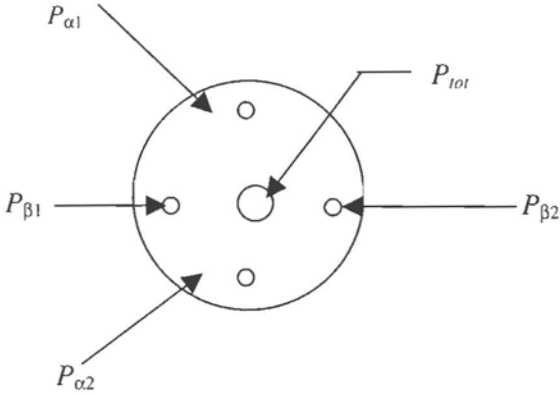


Figure 2. 5-Hole pressure ports configuration

$$\alpha_{Lo} = \frac{P_{\alpha1} - P_{\alpha2}}{K_{\alpha} P_{dyn}} \quad (1)$$

where  $K_{\alpha}$  is a sensitivity coefficient.

The differential pressure ( $p_{\beta1} - p_{\beta2}$ ) is proportional to the product of dynamic pressure ( $p_{dyn}$ ) times  $\beta_{Lo}$ , where the dynamic pressure equals local pitot pressure minus local static pressure and  $\beta_{Lo}$  equals local angle of sideslip. Local angle of sideslip,  $\beta_{Lo}$ , can be determined<sup>2</sup> according to the relationship:

$$\beta_{Lo} = \frac{P_{\beta1} - P_{\beta2}}{K_{\beta} P_{dyn}} \quad (2)$$

where  $K_{\beta}$  is a sensitivity coefficient.

Both angle of attack and angle of sideslip can be calibrated simultaneously. One of the methods adopted by Rosemount is used in the current study of 5-hole probe calibration. Figure 3 gives Rosemount calibration curve, ie, the linear sensitivity per degree,

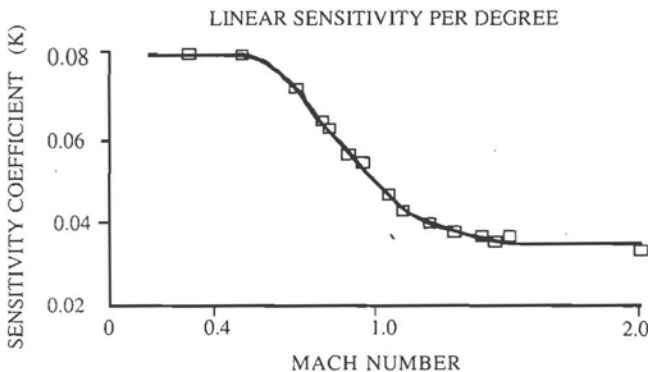


Figure 3. Rosemount calibration curve

as a function of Mach number. The sensitivity coefficient is the same for the factors  $K_{\alpha}$  and  $K_{\beta}$  (ie, for both angle of attack and angle of sideslip)<sup>3</sup>. From the above curve, it is observed that the sensitivity coefficient ( $K$ ) is constant up to Mach number roughly equal to 0.5. For higher Mach numbers up to the upper range of tested Mach number 0.6, slight effect of Mach number on the sensitivity coefficient is discernible.

### 3. FLIGHT-TEST PROGRAMME

As already pointed out, a comprehensive flight test with excitation of the longitudinal-and lateral-directional motion is carried out to calibrate the 5-hole probe. The flight tests are carried out in the gear up, nominal mid-centre of gravity configuration at three flight levels of 90, 160 and 240 which correspond to 2750 m, 4900 m and 7350 m, respectively. The nominal flight conditions or the test points are specified by settings of the landing flap ( $\delta_f$ ) and indicated air speed (KIAS). Two landing flap positions,  $\delta_f = IN$  and  $14^\circ$ , are selected for flight testing. Table 1 defines the flight test matrix at various airspeeds as a function of flap setting.

Table 1. Test flight conditions

KIAS	140	150	160	200	230	260
$\delta_f = IN$						
$\delta_f = 14^\circ$						

At flight conditions defined in Table 1, different flight manoeuvres (eg, 3-2-1-1 / doublet elevator input, doublet rudder input, pull up and push down, and steady sideslip manoeuvres) to excite the longitudinal-and lateral-directional motion are carried out.

### 4. ONBOARD MEASUREMENTS

An onboard measurement system installed in the test aircraft, ATTAS, provides measurements of a large number of signals, such as aircraft motion variables, atmospheric conditions, control surface positions, engine parameters, etc. Most of the signals are measured using dedicated sensors. In some cases,

measurements from the inertial platform and digital air data computer are used. The basic sampling rate of the measurement and the recording system is 50 Hz. A brief description of the measurements required for calibration of 5-hole probe is given.

The longitudinal, lateral, and vertical accelerations along the three body axes are measured using a dedicated accelerometer triad located near the centre of gravity. Dedicated rate gyros are used for the measurement of the angular rates. The measurements of attitude angles are obtained from the inertial platform. The 5-hole probe provides the raw measurements of differential pressure for  $\alpha$  and  $\beta$ . The dynamic pressure measurement is obtained from the total pressure and the static pressure. The measurements of altitude, static pressure, total pressure, and temperature are obtained from the digital air data computer. The fuel flow rate is measured and numerically integrated to provide a direct measure of the total fuel consumption. The flight instrumentation incorporates respective transducers and associated signal conditioning units. The various signal conditioning units include analog filters with a 32 Hz cutoff frequency.

## 5. PARAMETER ESTIMATION ALGORITHM

The dynamical system, whose parameters are to be estimated, is assumed to be described<sup>4,5</sup> by the following<sup>4,5</sup> general nonlinear equations:

$$\dot{x}(t) = f \begin{bmatrix} x(t), X(t, \tau), u(t) \\ -\Delta u(b_{u,l}), U(t, \tau), \beta \end{bmatrix} \quad x(t_{0,l}) = x_0(b_{x,l}) \quad (3)$$

$$y(t) = g \begin{bmatrix} x(t), X(t, \tau), u(t) \\ -\Delta u(b_{u,l}), U(t, \tau), \beta \\ + \Delta z(b_{y,l}) \end{bmatrix} \quad l = 1, 2, \dots, nz \quad (4)$$

$$z(t_k) = y(t_k) + G v_m(t_k) \quad k = 1, 2, \dots, N \quad (5)$$

where  $x$  is a  $(n \times 1)$  state vector,  $u$  the  $(p \times 1)$  control input vector and  $y$  the  $(m \times 1)$  model output or observation vector. The  $n$  and  $m$  are the dimensional system functions, and  $f$  and  $g$  are the general nonlinear real-valued vector functions. Measurements,  $Z$ , of these output variables that are corrupted with noise vector  $(v_m)$ , are available for  $N$  discrete sampling times  $t_k$ . The measurement noise vector, is assumed to be characterised by a sequence of independent Gaussian random variables with zero mean and identity covariance. The matrices  $X(t, \tau)$  and  $U(t, \tau)$  denote the matrices of the time-delayed state and input variables with

$$\begin{aligned} [X(t, \tau)]_{ij} &= x_i(t - \tau_j) \\ [U(t, \tau)]_{ij} &= u_i(t - \tau_j) - \Delta u(b_{u,l}) \end{aligned} \quad (6)$$

The postulated model includes  $nz$  time records to be analysed simultaneously. Further,  $\beta$  represents the unknown system coefficients,  $\tau$ , the unknown time delays;  $x_0$  the initial conditions,  $\Delta z$  and  $\Delta u$  the possible zero shifts in the measurements of the output and control variables. In general, not all of the components of  $x_0$ ,  $\Delta z$ ,  $\Delta u$  can be estimated since these may be linearly dependent or highly correlated. The corresponding components which can be estimated are denoted by for the  $l^{\text{th}}$  time segment, respectively. The unknown parameter vector  $\Theta$  in this case is given by

$$\Theta^T = \left\{ \beta^T; \tau^T; b_{x,1}^T, \dots, b_{x,nz}^T; b_{y,1}^T, \dots, b_{y,nz}^T; b_{u,1}^T, \dots, b_{u,nz}^T \right\} \quad (7)$$

The maximum likelihood estimates<sup>4,6</sup> of  $\Theta$  are obtained by minimising the negative logarithm of the likelihood function:

$$\begin{aligned} J(\Theta) &= \frac{1}{2} \sum_{k=1}^N [z(t_k) - y(t_k)]^T \\ &R^{-1} [z(t_k) - y(t_k)] + \frac{N}{2} \ln |R| \end{aligned} \quad (8)$$

where  $R$  is the covariance matrix of the residuals. An estimation algorithm based on Eqns (3)-(8)

accounts for measurement noise only and is often referred to as maximum likelihood output error algorithm. Such an algorithm is considered adequate in the current work mainly, because the flight tests carried out were in a fairly steady atmosphere<sup>6-8</sup>. This algorithm<sup>9</sup>, which is a part of ESTIMA, the integrated software for parameter estimation and simulation of dynamical systems, is applied to check the kinematic consistency of the measured flight data.

### 6. DATA COMPATIBILITY CHECK

The data compatibility check also called the flight path reconstruction is an integral part of aircraft parameter estimation. The aim is to ensure that the measurements are consistent and error-free. For example, the measured angle of attack must match with that reconstructed from the accelerometer and gyro measurements. Such a verification is possible in the case of flight data, because the well-defined kinematic equations of aircraft motion provide a convenient means to bootstrap the information through a numerical procedure. Since no uncertainties are involved in the kinematic model, the compatibility check provides an accurate information about the aircraft states. In addition, it provides the estimates of scale factors, zero shifts and time shifts in the recorded data.

The kinematic equations of aircraft motion are given by the following state equations:

$$\dot{u} = -(q - \Delta q)w + (r - \Delta r)v - g \sin \theta + (a_x - \Delta a_x), \quad u(0) = u_0$$

$$\dot{v} = -(r - \Delta r)u + (p - \Delta p)w + g \cos \theta \sin \phi + (a_y - \Delta a_y), \quad v(0) = v_0$$

$$\dot{w} = -(p - \Delta p)v + (q - \Delta q)u + g \cos \theta \cos \phi + (a_z - \Delta a_z), \quad w(0) = w_0$$

$$\dot{\phi} = (p - \Delta p) + (q - \Delta q) \sin \phi \tan \theta + (r - \Delta r) \cos \phi \tan \theta \quad \phi(0) = \phi_0$$

$$\dot{\theta} = (q - \Delta q) \cos \phi - (r - \Delta r) \sin \phi \quad \theta(0) = \theta_0$$

$$\dot{\psi} = (q - \Delta q) \sin \phi \sec \theta + (r - \Delta r) \cos \phi \sec \theta \quad \psi(0) = \psi_0$$

$$\dot{h} = u \sin \theta - v \cos \theta \sin \phi - w \cos \theta \cos \phi \quad h(0) = h_0 \quad (9)$$

The equations of aircraft motion used in the kinematic consistency checking is derived referred to the conventional aircraft body-fixed axes system<sup>1</sup>.

Observation equations are:

$$p_{\alpha m} = K_{\alpha} p_{dyn} \alpha_{Lo} - \Delta p_{d\alpha}$$

$$p_{\beta m} = K_{\beta} p_{dyn} \beta_{Lo} - \Delta p_{d\beta}$$

$$p_{dyn m} = \frac{1}{2} \rho V_{Lo}^2$$

$$\phi_m = K_{\phi} \phi + \Delta \phi \quad (10)$$

$$\theta_m = K_{\theta} \theta + \Delta \theta$$

$$\psi_m = K_{\psi} \psi + \Delta \psi$$

$$h_m = h + K_{h\alpha} \alpha_{Lo} + K_{h\beta} \beta_{Lo}$$

where  $p_{\alpha m}$  is equal to  $(p_{\alpha 1} - p_{\alpha 1})$  and  $p_{\beta m}$  is equal to  $(p_{\beta 1} - p_{\beta 2})$ .  $\alpha_{Lo}$  and  $\beta_{Lo}$  in Eqn (10) are in degrees. For parameter estimation purposes,  $p_{\alpha m}$  and  $p_{\beta m}$  in the observation equations [Eqn (10)] are obtained by rewriting Eqns (1) and (2). These are given by

$$\alpha_{Lo} = \tan^{-1} \left( \frac{w_{Lo}}{u_{Lo}} \right)$$

$$\beta_{Lo} = \sin^{-1} \left( \frac{v_{Lo}}{V_{Lo}} \right) \quad (11)$$

These are given by

$$\left. \begin{aligned} u_{Lo} &= u - (r - \Delta r)Y_{Lo} + (q - \Delta q)Z_{Lo} \\ v_{Lo} &= v - (p - \Delta p)Z_{Lo} + (r - \Delta r)X_{Lo} \\ w_{Lo} &= w - (q - \Delta q)X_{Lo} + (p - \Delta p)Y_{Lo} \end{aligned} \right\} (12)$$

Equation (10) for the observation variables are to be computed at each discrete time point. For the sake of brevity, the time dependance was not included in Eqn (10). The exact representation, for example, for the measured differential pressure for angle of attack ( $p_{\alpha m}$ ) with possible time delay is given by

$$p_{\alpha m}(t) = K_{\alpha} p_{dyn} \left( t - \tau_{dyn} \right) \alpha_{Lo} \left( t - \tau_{\alpha} \right) - \Delta p_{d\alpha} \quad (13)$$

The equation for differential pressure for angle of sideslip with time delay are incorporated in a similar manner. The measurements of Euler angles ( $\phi$ ,  $\theta$ ,  $\psi$ ) are likewise assumed to be biased with scale factors ( $K_{\phi}$ ,  $K_{\theta}$ ,  $K_{\psi}$ ) and zero shifts ( $\Delta\phi$ ,  $\Delta\theta$ ,  $\Delta\psi$ ). The observation equation for altitude includes two correction factors ( $K_{h_{\alpha}}$  and  $K_{h_{\beta}}$ ). This is to account for the rapid changes in  $\alpha$  and  $\beta$  due to dynamic manoeuvres.

In Eqn (9), the three linear accelerations ( $a_x$ ,  $a_y$ ,  $a_z$ ) and angular rates ( $p$ ,  $q$ ,  $r$ ) are the input variables, which are assumed to be biased. The kinematic equations are referred to a fixed point of the aircraft. In the present case, the aircraft centre of gravity is assumed to be the fixed point. For this reason, it is obvious that the input variables used in the state equations must be the measurements at the centre of gravity. In ATTAS, as pointed out earlier, the linear accelerometers are mounted not exactly at the centre of gravity, but at some convenient location near the range of centre of gravity. The exact accelerometer offset distances in a fixed reference frame is known. The centre of gravity location during the flight, accounting for the fuel

consumption, referred to the same axes system is obtained. From these two quantities, the actual offset distances,  $X_a, Y_a, Z_a$ , from the centre of gravity is computed. In a similar way, the offset distances from centre of gravity to any sensor is determined. The accelerations  $a_x, a_y$  and  $a_z$  at the centre of gravity are obtained from the accelerations  $a_{xa}, a_{ya}$  and  $a_{za}$  measured at a point away from the centre of gravity through the following relations:

$$a_x = a_{xa} + (q^2 + r^2) X_a - (pq - \dot{r}) Y_a - (pr + \dot{q}) Z_a \quad (14)$$

$$a_y = a_{ya} - (pq + \dot{r}) X_a + (r^2 + p^2) Y_a - (rp - \dot{p}) Z_a$$

$$a_z = a_{za} - (pr - \dot{q}) X_a - (qr + \dot{q}) Y_a + (p^2 + q^2) Z_a$$

The onboard instrumentation does not provide measurements of  $\dot{p}$ ,  $\dot{q}$  and  $\dot{r}$ . In Eqn (14), the angular accelerations obtained by numerical differentiation of the angular rates are used. Since the inertial measurements are usually of very high quality, the errors and noise due to numerical differentiation are expected to be negligible. Equations (9)-(14) are incorporated in a maximum likelihood estimation program to estimate the states and the unknown scale factors and zero shifts<sup>9</sup>. To avoid some drift in the integrated variables, biases in the measurements of the six input variables, although may be small, are always estimated. The scale factors and zero shifts in the Euler angles ( $\phi$ ,  $\theta$ ,  $\psi$ ) were found to be negligible. Thus, the following set of unknown parameters was considered adequate:

$$\Theta^T = \left[ \Delta a_x, \Delta a_y, \Delta a_z, \Delta p, \Delta q, \Delta r, K_{\alpha}, \Delta p_{d\alpha}, K_{\beta}, \Delta p_{d\beta}, K_{h_{\alpha}}, K_{h_{\beta}} \right] \quad (15)$$

In addition to the above unknown parameters, it is required to estimate the unknown initial conditions ( $u_0, v_0, w_0, \phi_0, \theta_0, \psi_0, h_0$ ).

7. DATA ANALYSIS

Point identification analysis is adopted to start with. The angle of attack and the angle of sideslip excitation manoeuvres with repeat runs at each flight test point are combined and the analysis is carried out using the maximum likelihood estimation algorithm. Accounting for the parameters as in Eqn (15), provided reasonable match for the observation variables. Figure 4 shows typical match between the measured and the estimated variables, namely differential pressure for angle of attack, differential pressure for angle of sideslip, dynamic pressure and altitude for a typical flight condition of flight level (FL) = 160, KIAS = 200,  $\delta_f = 1N$ . Time history of Mach number is also included in the figure. In Fig. 4, PD AL799 represents the differential pressure for angle of attack, PD BE800, the differential pressure for angle of sideslip, PSTAU801, the dynamic pressure, HQNEY, the altitude and MAY, and the Mach number. Also the

continuous lines in Fig. 4 represent the flight measured signal and the dashed lines represent the estimated ones. Although the overall match in terms of dynamic variations appears to be good, a closer look at the expanded time scale plots of differential pressure for angle of attack, differential pressure for angle of sideslip and dynamic pressure, indicate some discrepancies in time synchronisation. It is observed that the measured differential pressure for angle of attack, differential pressure for angle of sideslip, and dynamic pressure from the 5-hole probe lag those estimated by the kinematic model. Also, it is observed that the measurements of Euler angles, ( $\phi, \theta, \psi$ ) obtained from the inertial platform also lag those estimated by the kinematic model. Since, the physical system under investigation is casual and the flight tests are conducted in steady atmosphere, the discrepancies clearly indicate time lag in the measured quantities. It may be recalled, that the linear accelerations and angular rates are measured by dedicated accelerometers and rate gyros and also directly recorded, and hence these form the best reference point for time-delay estimation. Hence, these measurements are taken as the reference to compute time-delay in other variables.

Based on the foregoing discussions, it is now attempted to additionally estimate the time delays in the measured 5-hole probe pressures and Euler angles. Simultaneous estimation of the system parameters as well as time delays is possible with the estimation software package used in the current study<sup>9</sup>. Augmenting the parameter vector,  $\Theta$ , in Eqn (15) with time delays in differential pressure for angle of attack and angle of sideslip, dynamic pressure and Euler angles, and the data compatibility check has been carried out for various flight configurations. This results in the following set of unknown parameters to be estimated:

$$\Theta^T = \left[ \Delta a_x, \Delta a_y, \Delta a_z, \Delta p, \Delta q, \Delta r, K_\alpha, \Delta p_{d\alpha}, \tau_\alpha, K_\beta, \Delta p_{d\beta}, \tau_\beta, \tau_{p\ dyn}, \tau_\phi, \tau_\theta, \tau_\psi, K_{h_\alpha}, K_{h_\beta} \right] \quad (16)$$

In addition to the above unknown parameters, it is also required to estimate the unknown initial conditions ( $u_0, v_0, w_0, \phi_0, \theta_0, \psi_0, h_0$ ).

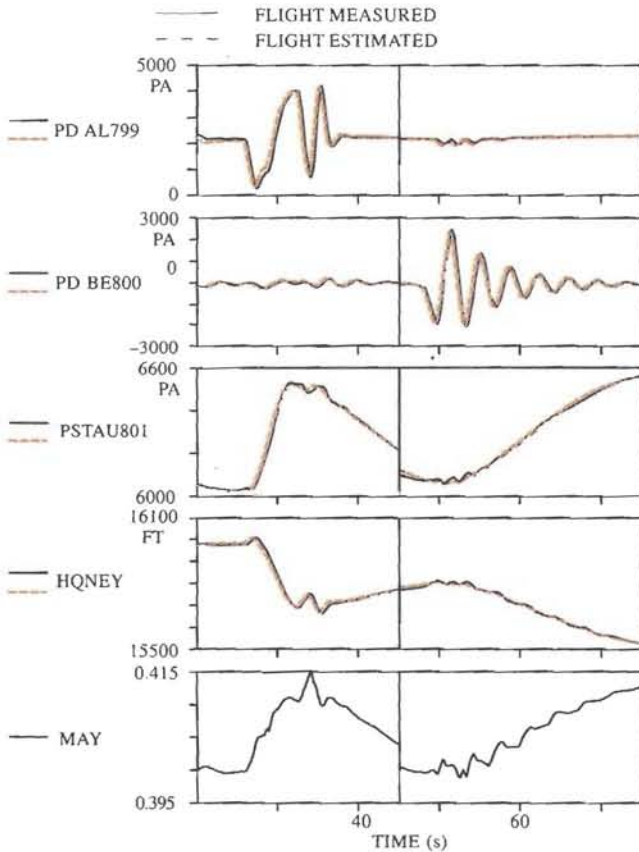


Figure 4. Data compatibility check (neglecting the time delays) FL 160, KIAS 200, FLAPS 1N.

The significantly improved match in Fig. 5 compared to Fig. 4 clearly indicates the need to account for the time delays in the recorded pressure measurements from the 5-hole probe and Euler angles. Repeated analysis with a number of different time records from various flights consistently led to the same conclusions. Estimates at nine typical flight conditions are provided in the Table 2. The time delay in differential pressure for angle of sideslip is nearly 130 ms for all runs, whereas in differential pressure for angle of attack, some scatter in time delay is observed. This could be due to the fact that the angle of sideslip oscillation persist for a longer period of 20 to 25 s in ATTAS whereas the angle of attack excitation lasts for a shorter duration. The time delay in the dynamic pressure cannot be estimated directly. The accurate measurement of dynamic pressure requires additional data on wind, etc. Since the dynamic pressure is from the same source as angle of attack and the angle of sideslip,

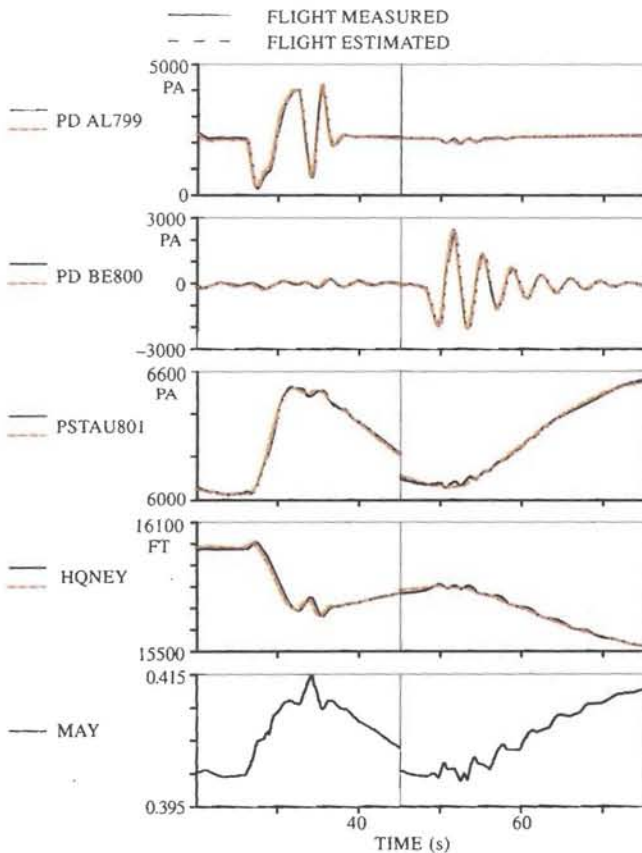


Figure 5. Data compatibility check (accounting for the time delays) FL 160, KIAS 200, FLAPS IN.

the time delay in dynamic pressure is fixed at the value of 130 ms for the subsequent runs. The time delays in  $\phi$ ,  $\theta$ , and  $\psi$  consistently estimated from different time segments, were 30 ms, 33 ms and 110 ms, respectively. These estimates of the time delay agree reasonably well with the specifications of the inertial platform as possible time delays due to the transport delays, filters, etc.<sup>10</sup>.

The estimates of biases in the input variables are small. The smaller values for the biases are expected, since the inertial measurements are, in general, of high accuracy. In contrast, the differential pressure measurements from 5-hole probe,  $p_{\alpha m}$  and  $p_{\beta m}$ , show consistently scale factor and zero-shift variations. In general, the scale factors estimated for differential pressure for angle of attack and angle of sideslip from different flights agree reasonably well, with a small scatter from record-to-record analysed. The estimates of zero-shift variation for differential pressure for angle of sideslip show a large scatter from record-to-record analysed. This is mainly due to the fact that the initial condition estimate of the velocity component,  $v$  and the zero-shift variations of differential pressure for angle of sideslip are highly correlated.

To correct the recorded flight data for measurement errors on a common basis, the data compatibility check is carried out by combining all the time records consisting of different flight test points (number of time segments analysed simultaneously,  $n_z = 32$  and number of data points,  $N = 21,822$ ) corresponding to FL = 90, 160, and for flap position  $\delta = IN$  in the estimation. The Mach number variation is between 0.23 to 0.53. The estimated values of the parameters are given in the Table 3 for the multiple manoeuvre analysis run. The estimate of scale factors and time delays for the angles of attack and sideslip are nearly the same. Subsequently, the data compatibility check is carried out in verification mode for all flight test points corresponding to a flap setting,  $\delta_f = 14^\circ$ . In the verification mode, all the parameters are fixed to the estimated value obtained corresponding to  $\delta_f = IN$ . Only the biases in the input variables and initial condition of the states are estimated. The trajectory match at a typical flight condition,

**Table 2. Estimates of scale factors and biases from data compatibility check**

	FL = 90			FL = 160				FL = 160	
	$\delta_f = IN$			$\delta_f = IN$				$\delta_f = 14^\circ$	
CIAS	150	200	230	150	200	230	260	140	160
Alt (m)	2730.0	2780.0	2780.0	4850.0	4860.0	4990.0	5036.0	4910.0	4970.0
Mach No	0.2680	0.3600	0.4100	0.3050	0.4000	0.4700	0.5300	0.2850	0.3300
$K_\alpha$	0.0750	0.0764	0.0834	0.0774	0.0822	0.0811	0.0800	0.0802	0.0838
	(2.0400)*	(2.5900)	(1.5000)	(0.7600)	(0.9000)	(1.2300)	(1.5300)	(1.2200)	(1.3400)
$\Delta p_{d\alpha}$ (Pa)	-283.8200	-340.2400	-137.7400	-99.2700	-130.2500	-180.9700	-91.5300	-152.6600	-96.6400
	(16.1300)	(15.7600)	(23.2300)	(17.1600)	(15.1700)	(14.8500)	(28.8300)	(7.6300)	(10.5800)
$\tau_\alpha$ (s)	0.1086	0.1450	0.1089	0.1108	0.1439	0.1111	0.1415	0.1408	0.1051
	(6.9600)	(8.1900)	(4.3100)	(2.4400)	(2.9400)	(3.5100)	(1.9700)	(2.9900)	(3.1600)
$K_\beta$	0.0797	0.0839	0.0817	0.0798	0.0820	0.0827	0.0817	0.0795	0.0811
	(2.0900)	(0.9000)	(1.0800)	(0.3700)	(0.2800)	(0.5700)	(0.6600)	(0.4600)	(0.3500)
$\Delta p_{d\beta}$ (Pa)	-645.4600	339.8800	406.2100	20.0800	-179.8000	536.8200	83.5300	26.9900	-208.4100
	(30.1900)	(73.3500)	(81.6000)	(299.4000)	(59.7800)	(30.1300)	(397.600)	(286.700)	(44.9900)
$\tau_\beta$ (s)	0.1549	0.1257	0.1307	0.1295	0.1314	0.1353	0.1461	0.1222	0.1331
	(9.6900)	(4.3500)	(4.3300)	(2.0600)	(1.2800)	(2.3900)	(2.0600)	(2.8300)	(1.8400)
$ R $	2.3' 10#	9.3' 10	1.5' 09	1.1' 12	1.9' 11	1.5' 10	1.3' 10	4.3' 11	1.8' 10

\* Values in parentheses indicate estimated standard deviations in percentage.

# The factor  $10^x$  is denoted as 'x.

namely FL = 160, 140 KIAS for the angles of attack and sideslip variations (repeat runs) are shown in Fig. 6. The predicted time history matches reasonably well with the flight measured.

Based on the *a-priori* information about Mach dependency from Fig. 3, the calibration of the 5-hole probe at Mach number 0.59 to 0.60 corresponding to FL = 240, KIAS = 260,  $\delta_f = IN$  carried out separately. To start with, data

compatibility check using parameter estimation method is carried out at this flight test point in verification mode. Parameters relating to angle of attack and angle of sideslip observables are fixed at the estimated values obtained from multiple run analysis, ie, Table 3. Only the initial condition of the states and biases in the input variables are estimated. The match between flight measured and predicted observables is satisfactory for  $\beta$ , indicating that the scale factor for  $\alpha$  appears to be Mach-

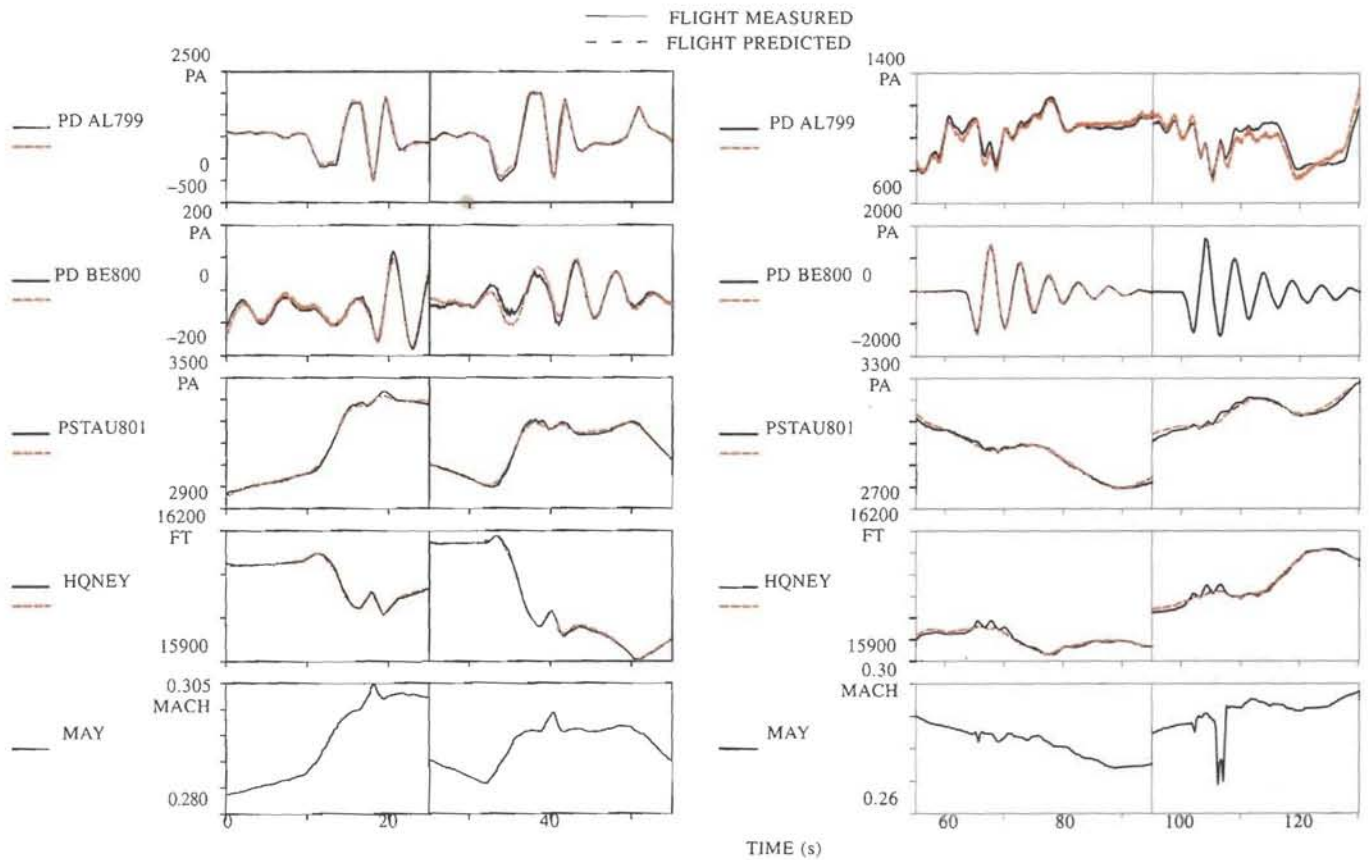


Figure 6. Data compatibility check-verification mode (flap = 14 °)

independent for the tested range. On the other hand, some small discrepancies in the  $\alpha$  are discernible. This suggests the effect of Mach number on  $\alpha$  measurement for Mach number beyond 0.53.

Table 3. Estimates of scale factors and biases from multiple run,  $\delta_j = IN$

FL = 90, 160 KIAS = 150, 200, 230, 260						
Parameters						
	$K_\alpha$	$\Delta p_{d\alpha}$	$\tau_\alpha$	$K_\beta$	$\Delta p_{d\beta}$	$\tau_\beta$
		(Pa)	(s)		(Pa)	(s)
$\delta_j = IN$	0.0819	-131.37	0.1406	0.0819	-199.62	0.1357
	(0.3400)	(10.2300)	(1.4500)	(0.3400)	(36.8200)	(1.4000)
$ R $	$1.6 \cdot 10^{-9}$ <sup>#</sup>					

\* Values in parentheses indicate estimated standard deviations in percentage

# The factor  $10^x$  is denoted as 'x'

Note that Rosemount calibration curves show Mach dependency for both  $\alpha$  and  $\beta$  beyond Mach number 0.53.

In the next step, data compatibility check is carried out at this test point to estimate the parameters relating to angle of attack and angle of sideslip observables. The parameter estimates for angle of attack and sideslip observables are given in Table 4. From the table, it is clear that the estimate of scale factor for  $\alpha$  is decreased to 0.0781 compared to an estimate of 0.0819 from multiple manoeuvre run analysis. The estimate of time delay for angle of side slip is increased to a value of 154.9 ms compared to an average estimate value of 135.7 ms from multiple manoeuvre run analysis. This correlates the dependency of scale factor for angle of attack with Mach number beyond 0.53. The estimated time delays in the difference pressures for angle of attack and angle of sideslip were crosschecked through post-calibration in the laboratory. Such laboratory calibration also indicated

**Table 4. Estimates of scale factor and bias for Mach number of about 0.59,  $\delta_f = IN$** 

FL = 240, KIAS = 260 (Altitude = 7122 m)						
Parameters						
	$K_\alpha$	$\Delta p_{d\alpha}$ (Pa)	$\tau_\alpha$ (s)	$K_\beta$	$\Delta p_{d\beta}$ (Pa)	$\tau_\beta$ (s)
$\delta_f = IN$	0.0781 (0.64)*	-131.37*	0.1415 (1.68)	0.0813 (0.31)	-199.62*	0.1549 (0.89)
$ R $	6.2' -11#					

\* Values in parentheses indicate estimated standard deviation in percentage.

# The factor  $10^x$  is denoted as 'x.

+ Values fixed from multiple manoeuvre analysis run.

time delay of 120 ms. Thus, the parameter estimation results match well with the laboratory calibration.

## 8. CONCLUSION

This paper describes the investigations carried out to calibrate the 5-hole probe for flow angles from ATTAS flight data. The flight tests were carried out with gear up and at nominal mid centre of gravity location for flap positions  $\delta_f = IN$  and  $\delta_f = 14^\circ$ . Dynamic manoeuvres were executed to excite the short period and dutch roll mode of the aircraft. The data compatibility check on the recorded flight data has been carried out using maximum likelihood output error algorithm to estimate the bias, scale factor, and time delay in the pressure measurements from 5-hole probe mounted on a noseboom in front of aircraft nose.

Through kinematic consistency checking, flight-validated scale factors, biases and time delays are determined for the differential pressure measurements for the angle of attack and the angle of sideslip. Also, the dynamic pressure measurement is found to have time delay. It is once again confirmed from the earlier investigations that the measurements of attitude angles obtained from the inertial platform clearly indicate time delay referred to the other signals, like linear accelerations and angular rates which are measured with the dedicated flight

instrumentation package. The identified time delays in attitude angles agreed well with the inertial platform specifications. The estimates of sensitivity coefficients, scale factors, from the flight data analysis correlate reasonably well with the manufacturer Rosemount calibration curves for the tested Mach range 0.23 to 0.53. The flight data analysis at Mach number 0.59 indicates Mach dependency for the angle of attack.

## ACKNOWLEDGEMENTS

This investigation was carried under DLR-NAL collaborative exchange programme. Shri V. Parameswaram (author) gratefully acknowledges Prof Dr P. Hamel, the then Director DLR, Institute of Flight Research, Braunschweig, Germany and Dr T.S. Prahalad, Director, National Aerospace Laboratories, Bangalore, for their encouragement. The authors would like to thank all those members of the Simulation and Flight Test Technique Branches, who have directly or indirectly contributed to this programme, particularly H. H. Lange and A. Zach deserve special mentioning. The authors also express their appreciation to Sarvashri S. Seydel, Chief Test Pilot, M. Preß, the Flight Test Engineer, from the Flight Test Centre of DLR in Braunschweig for out most efficiently carrying flight test manoeuvres for the calibration of 5-hole probe flow angles on ATTAS aircraft.

## REFERENCES

1. Jategaonkar, R. V. Identification of the aerodynamic model of the DLR research aircraft ATTAS from flight test data. Report No. DLR-FB 90-40, July 1990.
2. Rosemount Inc, Aerospace Division, Burnsville, Minnesota 55337, Rosemount Model 858 flow angle sensors. Bulletin 1014, Minnesota, U.S.A.
3. De Leo, R.V. & Hagen, F.W. Aerodynamic performance of Rosemount model 858AJ air data sensor. Rosemount Report No. 8767, July 1976, Minnesota, U.S.A.
4. Jategaonkar, R. V. & Plaetschke, E. Maximum-likelihood parameter estimation from flight test

- data for general nonlinear systems. Report No. DFVLR-FB, 83-14, April 1983.
5. Plaetschke, E. Ein FORTRAN-programm zur maximum-likelihood-parameterschätzung in nichtlinearen retardierten systemen der flugmechanik-benutzeranleitung. Report No DFVLR-Mitt. 86-08, March 1986 (German).
  6. Evans, R. J.; Goodwin, G. C.; Feik, R. A.; Martin, C. & Lozano-Leal, R. Aircraft flight data compatibility checking using maximum likelihood and extended Kalman filter estimation. *In* Proceeding of the 7<sup>th</sup> IFAC Symposium: Identification and System Parameter Estimation, York, UK, July 1985. pp. 487-92.
  7. Keskar, D. A. & Klein, V. Determination of instrumentation errors from measured data using maximum likelihood method. American Institute of Aeronautics and Astronautics, USA. AIAA Paper No. 80-1602, 1980.
  8. Jategaonkar, R.V. & Plaetschke, E. Maximum likelihood estimation of parameters in linear systems with process and measurement noise. Report No. DFVLR FB 87-20, June 1987.
  9. Jategaonkar, R.V. ESTIMA: A modular and integrated software tool for parameter estimation and simulation of dynamic systems—users's manual, version 1.0. Report No DLR-IB 111-2001/29, July 2001.
  10. N.N. Technical Description of LTN-90 Inertial reference system. No. 502006, Aero products, California, U.S.A., January 1983.

#### Contributor



**Mr V. Parameswaran** obtained his MS from the Indian Institute of Technology (IIT) Madras, Chennai, in 1989. Presently, he is working as Senior Scientist at the Flight Mechanics and Control Division of the National Aerospace Laboratories (NAL), Bangalore. His areas of research include: Instrumentation, modelling and parameter estimation of aerospace vehicles, and GPS-related activities. He was on deputation to Braunschweig, Germany, as Guest Scientist from March to December 1989 and April to September 2001. He is a member of the Institution of Engineers (India) and the Aeronautical Society of India.